Journal of Asian Ceramic Societies 2 (2014) 195–198

Contents lists available at ScienceDirect

Journal of Asian Ceramic Societies

journal homepage: www.elsevier.com/locate/jascer

Letter

Novel environment-friendly inorganic red pigments based on $(Bi, Er, Y, Fe)_2O_3$ solid solutions

ARTICLE INFO

Keywords:
Bismuth oxide
Environment-friendly
Red pigment
Solid solution
Cubic δ-Bi_2O_3 structure
Solid-state reaction

ABSTRACT

Novel environmental-friendly inorganic red pigments, $((Bi_{0.72}Er_{0.28-x}Y_x)_{1-y}Fe_y)_2O_3$ ($0 < x \leq 0.28$, $y = 0.20$), were successfully synthesized using a conventional solid-state reaction method in order to further enhance the red hue of a $((Bi_{0.72}Er_{0.28})_{0.80}Fe_{0.20})_2O_3$ pigment, which was previously reported by our group. The color of the samples depended on their composition and the most brilliant red hue was obtained for $((Bi_{0.72}Er_{0.04}Y_{0.24})_{0.80}Fe_{0.20})_2O_3$. The a^* value corresponding to red chromaticity was +33.1 for $((Bi_{0.72}Er_{0.04}Y_{0.24})_{0.80}Fe_{0.20})_2O_3$, and it was greater than those of previously reported $((Bi_{0.72}Er_{0.28})_{0.80}Fe_{0.20})_2O_3$ ($a^* = +30.9$) and commercial Fe_2O_3 ($a^* = +28.9$) pigments. Since the $((Bi_{0.72}Er_{0.04}Y_{0.24})_{0.80}Fe_{0.20})_2O_3$ pigment is composed of nontoxic elements (Bi, Er, Y, Fe, and O), it should be an attractive alternative to the conventional Fe_2O_3 pigments.

1. Introduction

Inorganic pigments are applied in a wide variety of products such as paints, ceramics, plastics, enamels, and glasses, because they possess high thermal and UV stability [1]. In particular, inorganic red pigments are in demand because of their wide applicability. Several inorganic red pigments such as lead oxides (red lead; Pb_3O_4 or $2PbO{\cdot}PbO_2$), cadmium sulfoselenide red (CdSe·CdS), and mercuric sulfide red (HgS) were popularly used for many applications. However, the use of these compounds has been restricted because of the hazardous elements, such as lead (Pb), cadmium (Cd), and mercury (Hg), which are harmful not only to human health but also to the environment. On the other hand, iron oxide (Fe_2O_3) has been widely known as an environmentally friendly inorganic red pigment for many uses, but its color performance is unsatisfactory in comparison to those of the conventional toxic pigments. A number of studies have been done on new environmentally friendly inorganic red pigments [2–9], but the pigments cannot exceed the color of the nontoxic red iron oxide (Fe_2O_3). Although perovskite-type oxynitrides $Ca_{(1-x)}La_xTaO_{(2-x)}N_{(1+x)}$ have also been reported as nontoxic inorganic red pigments, toxic ammonia gas is required for the synthesis of these pigments [10]. Furthermore, oxidation of these oxynitride compounds occurs at 420 °C or higher temperatures [10], where they decompose and generate toxic nitrogen oxides.

Because of this situation, we focused on bismuth oxide (Bi_2O_3), which has already been reported as a nontoxic and insoluble compound [11]. Bi_2O_3 exists in several polymorphic phases: a low-temperature stable α-phase (monoclinic structure), a high-temperature stable δ-phase (cubic fluorite structure), and a metastable β-phase (tetragonal structure) or γ-phase (body-centered cubic structure). At room temperature, Bi_2O_3 exists in a pale yellowish α-phase, which is stable up to 730 °C. At around 730 °C, a phase transition from the α-phase to the orange δ-phase occurs, and the δ-phase is stable up to the melting point (825 °C). The color of Bi_2O_3 originates in the charge-transfer transition from the valence band of a hybrid orbital of Bi6s and O2p to the conduction band of Bi6p [12].

In our previous study, we elucidate that the high-temperature δ-Bi_2O_3 phase was stabilized at room temperature by introducing Er^{3+} ions into the Bi^{3+} site, and that the red chromaticity was significantly increased by further dissolution of Fe^{3+} into the lattice to insert the Fe3d level as a new energy level below the Bi6P conduction band. In particular, it was found that a $((Bi_{0.72}Er_{0.28})_{0.80}Fe_{0.20})_2O_3$ pigment showed the highest redness value ($a^* = +30.9$ in the CIE $L^*a^*b^*$ system) [13]. However, the band gap energy of the $((Bi_{0.72}Er_{0.28})_{0.80}Fe_{0.20})_2O_3$ pigment became too low because of significant lattice shrinkage, and the optical absorption extended into the red region. As a result, the red color was not so vivid, although it was higher than that of the commercial Fe_2O_3 pigment ($a^* = +28.9$) [13]. In this study, therefore, a part of the Er^{3+} (0.103 nm) [14] site was substituted with larger Y^{3+} ions (0.104 nm) [14] to relax the excessive lattice shrinkage. Therefore, $((Bi_{0.72}Er_{0.28-x}Y_x)_{1-y}Fe_y)_2O_3$ ($0 < x \leq 0.28$, $y = 0.20$) samples were synthesized as advanced environmentally friendly red pigments. The color properties were characterized and the composition was optimized to produce the most vivid red hue.

Peer review under responsibility of The Ceramic Society of Japan and the Korean Ceramic Society.

Production and hosting by Elsevier

2187-0764 © 2014 The Ceramic Society of Japan and the Korean Ceramic Society. Production and hosting by Elsevier B.V. All rights reserved.
http://dx.doi.org/10.1016/j.jascer.2014.06.005

2. Experimental

The $((Bi_{0.72}Er_{0.28-x}Y_x)_{1-y}Fe_y)_2O_3$ $(0 < x \leq 0.28,\ y = 0.20)$ pigments were synthesized using a conventional solid-state reaction method. As is the case with the $((Bi_{0.72}Er_{0.28})_{0.80}Fe_{0.20})_2O_3$ pigment [13], double calcination was adopted in the synthesis process to obtain the $((Bi_{0.72}Er_{0.28-x}Y_x)_{1-y}Fe_y)_2O_3$ solid solutions certainly. In the first process, $(Bi_{0.72}Er_{0.28-x}Y_x)_2O_3$ solid solutions were prepared in a single-phase form of the cubic δ-Bi_2O_3 structure, and in the second one, Fe^{3+} ions were introduced into the $(Bi_{0.72}Er_{0.28-x}Y_x)_2O_3$ lattice maintaining the single-phase δ-Bi_2O_3 structure. Stoichiometric amounts of Bi_2O_3, Er_2O_3 and Y_2O_3 powders were mixed in an agate mortar, followed by mechanical mixing using a planetary-type ball-milling apparatus (Pulverisette 7, Fritsch GmbH) for 3 h. The homogenous mixed powder was calcined at 800 °C for 10 h under an air atmosphere. Finally, the powder obtained was mixed with Fe_2O_3 in an agate mortar and was calcined at 500 °C for 10 h under an air atmosphere.

All the samples were gently ground in an agate mortar before characterization. The sample compositions were analyzed by X-ray fluorescence spectroscopy (XRF, Rigaku Supermini200). The samples were characterized by X-ray powder diffraction (XRD; Rigaku, SmartLab) using Cu-Kα radiation (40 kV, 30 mA) to identify the crystal structure. Optical reflectance spectra were obtained using a UV–vis spectrometer (Shimadzu UV-2600) with barium sulfate as a reference. The band-gap energies of the samples were determined from the absorption edge of the absorbance spectra represented by the Kubelka–Munk function, $f(R) = (1-R)^2/2R$, where R is the reflectance [15,16]. The color properties of the samples were estimated in terms of the CIE $L^*a^*b^*$ system with a colorimeter (Konica-Minolta CR-300). The parameter L^* represents the brightness or darkness of a color relative to a neutral gray scale, while the parameters a^* (the red–green axis) and b^* (the yellow–blue axis) qualitatively express the color. The particle morphology of the samples was observed using a scanning electron microscope (SEM; Shimadzu, SS-550). The size distribution and mean particle size were evaluated by measuring the diameters of 200 particles on the SEM micrographs.

3. Results and discussion

The compositions of all samples determined by the XRF analysis were in good agreement with the theoretical values. To confirm the formation of the cubic δ-Bi_2O_3 structure, the $(Bi_{0.72}Er_{0.28-x}Y_x)_2O_3$ $(0 < x \leq 0.28)$ samples, which were synthesized in the first step of the double calcination process, were measured using the XRD analysis. Fig. 1 shows the XRD patterns of the $(Bi_{0.72}Er_{0.28-x}Y_x)_2O_3$ $(0 \leq x \leq 0.28)$ samples. A single phase of the δ-Bi_2O_3-type structure was observed for all samples, and there were no extra lines due to other compounds or impurities. As summarized in Table 1, the cubic lattice parameter of the $(Bi_{0.72}Er_{0.28-x}Y_x)_2O_3$ $(0 \leq x \leq 0.28)$ samples increased linearly with increasing the amount of Y^{3+}, because the ionic radius of Y^{3+} (0.104 nm) [14] is slightly larger than that of Er^{3+} (0.103 nm) [14]. These results indicate that the solid solutions were formed successfully for all samples.

Table 1
Cubic lattice parameters of the $(Bi_{0.72}Er_{0.28-x}Y_x)_2O_3$ $(0 \leq x \leq 0.28)$ samples with estimated standard deviation (esd).

Sample	Lattice parameter/nm
$(Bi_{0.72}Er_{0.28})_2O_3$ [13]	0.54843(23)
$(Bi_{0.72}Er_{0.18}Y_{0.10})_2O_3$	0.54891(17)
$(Bi_{0.71}Er_{0.10}Y_{0.19})_2O_3$	0.54934(42)
$(Bi_{0.72}Er_{0.04}Y_{0.24})_2O_3$	0.54950(81)
$(Bi_{0.72}Y_{0.28})_2O_3$	0.54982(25)

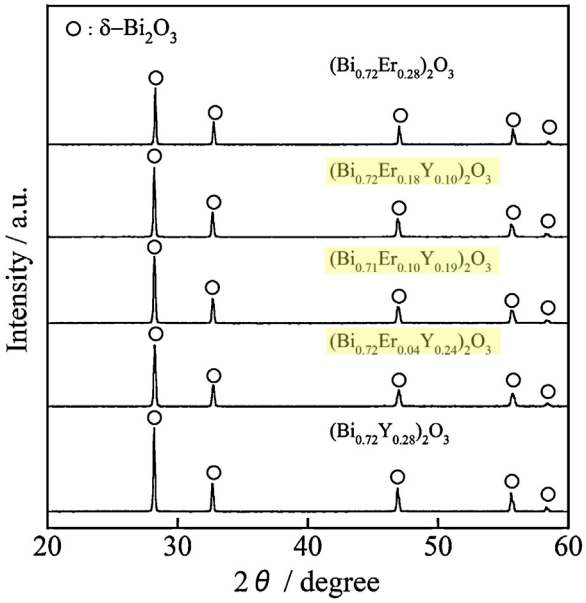

Fig. 1. XRD patterns of the $(Bi_{0.72}Er_{0.28-x}Y_x)_2O_3$ $(0 \leq x \leq 0.28)$ samples.

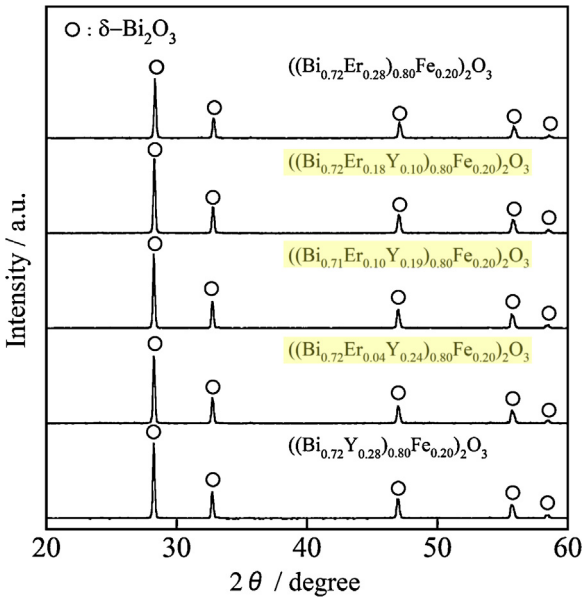

Fig. 2. XRD patterns of the $((Bi_{0.72}Er_{0.28-x}Y_x)_{1-y}Fe_y)_2O_3$ $(0 \leq x \leq 0.28,\ y = 0.20)$ samples.

Subsequently, iron ion (Fe^{3+}) was doped into the $(Bi_{0.72}Er_{0.28-x}Y_x)_2O_3$ lattice to introduce a red chromogenic species, and the XRD patterns of the $((Bi_{0.72}Er_{0.28-x}Y_x)_{1-y}Fe_y)_2O_3$ $(0 \leq x \leq 0.28,\ y = 0.20)$ samples were depicted in Fig. 2. Also in this case, a single-phase cubic δ-Bi_2O_3 structure was observed for all samples and no diffraction peaks of impurities were evident in the patterns. The cubic lattice parameters of $((Bi_{0.72}Er_{0.28-x}Y_x)_{1-y}Fe_y)_2O_3$ are summarized in Table 2. It is confirmed that the lattice parameters of the $((Bi_{0.72}Er_{0.28-x}Y_x)_{1-y}Fe_y)_2O_3$ samples were larger than that of $((Bi_{0.72}Er_{0.28})_{0.80}Fe_{0.20})_2O_3$ [13] and were increased with increasing Y^{3+} content. These results indicate that solid solutions were successfully formed for the $((Bi_{0.72}Er_{0.28-x}Y_x)_{1-y}Fe_y)_2O_3$ $(0 < x \leq 0.28,\ y = 0.20)$ samples, as is the case with the $(Bi_{0.72}Er_{0.28-x}Y_x)_2O_3$ samples in Table 1.

Fig. 3 shows the UV–vis diffuse reflectance spectra for the $((Bi_{0.72}Er_{0.28-x}Y_x)_{1-y}Fe_y)_2O_3$ $(0 \leq x \leq 0.28, y = 0.20)$ samples. Strong